

Probabilistic modelling of water balance at a point: the role of climate, soil and vegetation

BY I. RODRIGUEZ-ITURBE¹, A. PORPORATO², L. RIDOLFI²,
V. ISHAM³ AND D. R. COX⁴

¹*Environmental Engineering and Water Resources Program and Princeton
Environmental Institute, Princeton, NJ 08544, USA*

²*Dipartimento di Idraulica Trasporti e Infrastrutture Civili, Politecnico di Torino,
Corso Duca degli Abruzzi, 24, 10129 Torino, Italy*

³*Department of Statistical Science, University College London, Gower Street,
London WC1E 6BT, UK*

⁴*Nuffield College, University of Oxford, Oxford OX1 1NF, UK*

Received 2 July 1998; revised 21 December 1998; accepted 1 April 1999

The soil moisture dynamics under seasonally fixed conditions are studied at a point. The water balance is described through the representation of rainfall as a marked Poisson process, which in turn produces an infiltration into the soil dependent on the existing level of soil moisture. The losses from the soil are due to evapotranspiration and leakage, which are also considered dependent on the existing soil moisture. The steady-state probability distributions for soil moisture are then analytically obtained. The analysis of the distribution allows for the assessment of the role of climate, soil and vegetation on soil moisture dynamics. Further hydrologic insight is obtained by studying the various components of an average water balance. The realistic representation of the processes acting at a site and the analytical tractability of the model make it well suited for further analyses that consider the spatial aspect of soil moisture dynamics.

Keywords: marked Poisson process; soil moisture; stochastic models in hydrology

1. Introduction

A problem of fundamental hydrologic interest is the dynamic linkage between climate, soil and vegetation through the spatial and temporal variability of soil moisture. The driving elements of these dynamics are heavily dependent on the space and time-scales at which the system is observed. The strong and fundamental spatial character of the phenomenon is obvious, since soil moisture at any site is influenced by the distribution of precipitation and by competition from neighbouring vegetation. Moreover, the rainfall input itself may or may not be a function of the soil moisture depending on the size of the region being considered (Rodriguez-Iturbe *et al.* 1991; Entekhabi & Rodriguez-Iturbe 1994). When large continental scales are considered, precipitation needs to be made dependent on the existing soil moisture since the regional feedback becomes an important factor in the dynamics. From the temporal

point of view both the climatic characteristics and the vegetation response vary seasonally.

This paper concentrates on the study of the soil moisture dynamics at a point under seasonally fixed conditions. Thus climatic and vegetation characteristics are assumed to be representative of a particular season. The determination of the probabilistic behaviour of soil moisture under that framework, with a stochastic input of rainfall and realistic responses of soil and vegetation, is the necessary first step for further studies where the spatial dynamics are explicitly taken into account. The combination of a stochastic input of rainfall, which produces an infiltration that is a function of the moisture state of the soil, with losses from the soil that are also a function of the state, makes the problem especially challenging. Previous studies along the same lines have not considered simultaneously the stochastic input into the system and the output from it as a function of the present state. Relevant to this investigation are the papers by Milly (1993) and, particularly, by Cox & Isham (1986). Milly (1993) considered the stochasticity of precipitation in deriving the probability distribution of soil moisture but losses from evapotranspiration and leakage were assumed independent of soil water content. The analysis of Cox & Isham (1986), on which this paper is based, does not account for the upper bound which saturation imposes on the soil moisture.

We will consider dynamics that represent the physical process at a daily time-scale. Thus no attempt is made to model the internal structure of precipitation events, which are simply represented by a total depth of rain assumed to be concentrated at an instant in time. The losses from evapotranspiration and leakage are represented through a simple and commonly used scheme that is considered valid for temporal scales equal to or larger than one day (Eagleson 1982). Since it is hydrologically important to differentiate between the soil moisture regimes that imply stress on the vegetation and those that carry no stress, the evapotranspiration function incorporates such a transition. The model parameters will not be functions of time and thus the analysis represents conditions appropriate to a single season. Also the lack of internal structure in rainfall makes the interpretation of results valid only for time-intervals of the order of one day. The paper does not consider spatial dynamics and thus it should be seen as a first step towards a more complete analysis where competition for soil moisture takes place among neighbouring vegetation.

The paper starts with a description of the soil moisture balance equation at a point and the hydrologic importance of its different terms, including the probabilistic representation of the rainfall input and the state-dependent losses for evapotranspiration and leakage. It proceeds to derive the steady-state probability density function of soil moisture and the impact of climate, soil and vegetation in this distribution.

2. Soil moisture balance equation

Under conditions where there are no lateral contributions, the soil moisture balance equation at a point is expressed as

$$nz \frac{ds}{dt} = I(s, t) - E(s, t) - L(s, t), \quad (2.1)$$

where n is the porosity; z is the depth of soil; s is the relative soil moisture content; $I(s, t)$ is the rate of infiltration from rainfall; $E(s, t)$ is the rate of evapotranspiration; and $L(s, t)$ is the rate of leakage or deep infiltration. The total volume of soil is

given by the sum of the volumes of air, water and mineral components, i.e. $V_s = V_a + V_w + V_m$. The porosity is then defined as

$$n = \frac{V_a + V_w}{V_s}. \quad (2.2)$$

The volumetric water content, θ , is the ratio of water volume to soil volume and the relative soil moisture is then

$$s = \frac{V_w}{V_a + V_w} = \frac{\theta}{n}, \quad (2.3)$$

so that $0 \leq s \leq 1$. Throughout this paper we will use the normalized version of equation (2.1), where all terms are divided by nz .

(a) *Infiltration from rainfall*

We idealize the occurrence of rainfall as a series of point concentrations in continuous time arising in a Poisson process of rate λ . This corresponds, for example, to a process considered on a time-scale (e.g. daily) that is long relative to the durations of rain events, with all the rain effectively concentrated at, say, the start of the event. Thus the temporal structure within each rain event is ignored, as is subdaily variation in the loss of moisture from the soil. Each rain event is assumed to have a random depth, R , characterized by an exponential probability density function

$$f_R(r) = \alpha e^{-\alpha r}, \quad \text{for } r \geq 0, \quad (2.4)$$

where $1/\alpha$ is the mean depth of rain events. Interception can be included as discussed below.

In what follows we will refer to the normalized version of equation (2.4):

$$f_H(h) = \gamma e^{-\gamma h}, \quad (2.5)$$

where $H = R/nz$ and $\gamma = \alpha nz$, where s and h are both dimensionless.

The increment in soil moisture resulting from rainfall infiltrating the soil from a particular rain event is assumed to be equal to the standardized depth (H), when the soil has enough available storage to accommodate it. Whenever the rainfall depth exceeds the available storage, the excess water is converted to surface run-off. We are therefore assuming the common ‘saturation from below’ mechanism for run-off generation, studied in detail by Dunne (1978), albeit with no lateral distribution and excluding Hortonian overland flow. Thus the infiltration from a rain event occurring at a time $t+$ when the soil moisture level, $S(t)$, at time t is s , is a random variable, Y , taking values between 0 and $1 - s$ with probability density function

$$b(y; s) = \gamma e^{-\gamma y} + \delta(y - 1 + s) \int_{1-s}^{\infty} \gamma e^{-\gamma u} du, \quad (2.6)$$

where $\delta(\cdot)$ is the Dirac delta function. The distribution is shown in figure 1 where the mass at $(1 - s)$ represents the probability that a storm will produce saturation when the soil has moisture s .

It is important to notice that the above framework allows for the explicit consideration of losses due to interception, i.e. the part of rainfall that is intercepted by

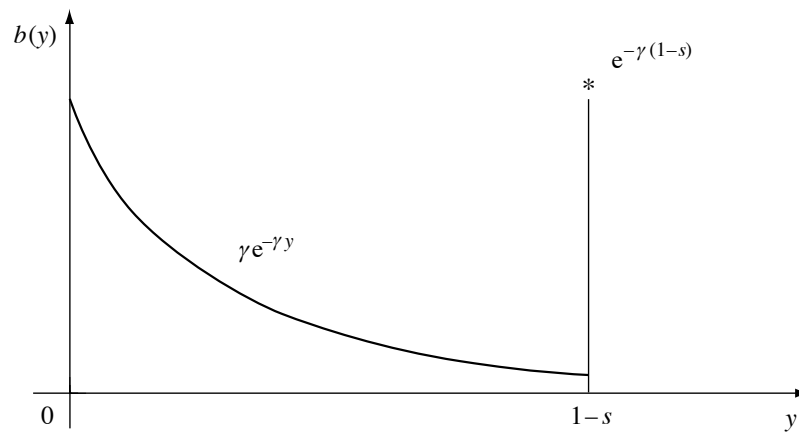


Figure 1. Sketch of the probability density function describing infiltration from rainfall. The * represents the atom of probability corresponding to soil saturation.

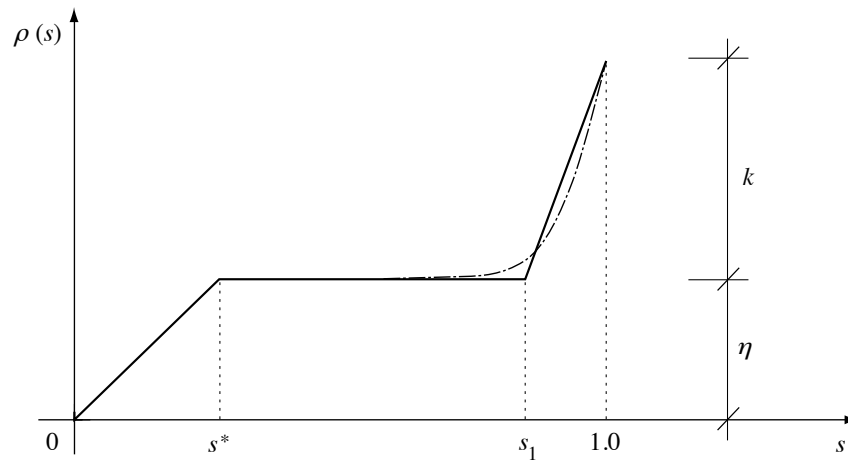


Figure 2. Schematic representation of the function used to model evapotranspiration and leakage losses (solid line). Also shown for comparison (dashed line) is the curve resulting from the use of equation (2.8) to model the leakage losses.

vegetation and evaporates before reaching the soil. In principle, interception depends on many factors such as intensity and duration of rainfall, type and degree of canopy coverage, temperature, etc. It is usually estimated through empirical relationships that vary from region to region. A common representation of interception at a given site is based on the estimation of a threshold for rainfall depth, δ , below which it is assumed that effectively no water will reach the ground. For modelling purposes the rainfall process is thus transformed to a new marked Poisson process where the rate of rainfall events is now $\lambda' = \lambda P[R > \delta] = \lambda e^{-\alpha\delta}$ and the depths, R' , have the same distribution as $R - \delta$, conditionally upon $R > \delta$. It follows that the density of R' is the same as that of R and is described by equation (2.4).

(b) *Evapotranspiration and leakage losses*

We will use a simplified but commonly accepted dependence of evapotranspiration on soil moisture. The functional relationship is shown in figure 2. The losses from evapotranspiration are assumed to increase linearly as a function of s until the moisture reaches a threshold, s^* , above which the evapotranspiration takes place at a maximum value, η , which for given climatic conditions depends on the type of vegetation—or lack of it—on the site. We assume representative climatic conditions, like ambient temperature and wind, that when coupled with the vegetation at the site yield the value of η . The threshold s^* depends heavily on the type of vegetation existing at the site and, in fact, for $s < s^*$ it is commonly assumed that the plant is under stress resulting from water deficit (Eagleson 1982). The value of s^* is considerably lower than the field capacity (the soil moisture level at which a particular type of soil stops draining by gravity, so that further depletion only takes place through evapotranspiration) and has been estimated from field experiments for different types of plants (see, for example, Scholes & Walker 1993). For notational convenience, in the following we will use E for the non-normalized maximum evapotranspiration, i.e. $E = \eta nz$.

Losses from leakage are a maximum, and, under the common assumption of a unit hydraulic gradient at the base of the soil profile, can be set equal to the saturated hydraulic conductivity of the soil, K_s , when the soil is saturated ($s = 1$). For $s < 1$ these losses decrease according to an experimentally determined power law (see, for example, Clapp & Hornberger 1978):

$$K(s) = K_s s^c, \quad (2.7)$$

where the exponent c depends on the type of soil and can vary from $c \simeq 11$ for sand to $c \simeq 25$ for clay. The normalized losses are then

$$z(s) = k s^c, \quad (2.8)$$

with $k = K_s/nz$. Equation (2.8) is approximated in our analysis by linear segments, as shown in figure 2, where the value of s_1 depends on the type of soil. This approximation is quite close in terms of the results it produces, but the value of s_1 should not be strictly interpreted as the field capacity of the soil.

The total normalized losses from the system are then given by the expression

$$\rho(s) = \frac{E(s)}{nz} + \frac{L(s)}{nz} = \begin{cases} \frac{\eta}{s^*} s, & 0 \leq s \leq s^*, \\ \eta, & s^* < s \leq s_1, \\ \eta + k \frac{s - s_1}{1 - s_1}, & s_1 < s \leq 1. \end{cases} \quad (2.9)$$

3. Probabilistic description of the dynamics

We now proceed to derive in detail the forward differential equations that relate the state probabilities at different points in time. Suppose that at time t the soil moisture level is $s(t)$ and consider a small time-interval from t to $t + dt$. The probability that no positive increment in soil moisture occurs is $1 - \lambda dt + o(dt)$. In this case

$$s(t + dt) = \begin{cases} s(t) - \Delta s, & \Delta s < s(t), \\ 0, & \Delta s \geq s(t), \end{cases} \quad (3.1)$$

where

$$\Delta s = \int_t^{t+dt} \rho(s(\tau)) d\tau = \rho(s(t)) dt + o(dt).$$

The probability that a positive increment in soil moisture takes place is $\lambda dt + o(dt)$. In this case

$$s(t+dt) = \begin{cases} s(t) + Y - \Delta s, & \Delta s < s(t) + Y, \\ 0, & \Delta s \geq s(t) + Y, \end{cases} \quad (3.2)$$

where Y is the normalized soil moisture increment described by the probability distribution $b(y; s(t))$ in equation (2.6). Since rainfall is modelled as instantaneous pulses we neglect the fact that evapotranspiration is inhibited throughout the duration of precipitation events.

At time t the distribution of $S(t)$ consists of a discrete atom of probability $p_0(t)$ that the soil is totally dry and a density $p(s, t)$ for $s > 0$. We note that if $S(t+dt) = s$ then, in the absence of any rainfall in $(t, t+dt)$,

$$S(t) = s + \rho(s) dt + o(dt) = s + \Delta s + o(dt),$$

for $s + \rho(s) dt$ decays by $\rho(s + \rho(s) dt) dt = \rho(s) + o(dt)$ in this time-interval. The probability that the soil moisture takes a value in $(s, s+ds)$ at the time $t+dt$ can therefore be expressed as follows (see, for example, Cox & Miller 1965, p. 241):

$$\begin{aligned} p(s, t+dt) ds &= (1 - \lambda dt) p(s + \Delta s, t) d(s + \Delta s) \\ &\quad + \lambda dt \int_0^s p(z + \Delta z, t) b(s - z; z) d(z + \Delta z) ds \\ &\quad + \lambda dt p_0(t) b(s; 0) ds + o(dt), \end{aligned} \quad (3.3)$$

where the second term on the right-hand side above allows for the case when the soil moisture reaches s due to a positive increment resulting from the arrival of a rainfall event, and the third term corresponds to when the process is at $s = 0$ at time t and the arrival of a storm event makes the moisture level jump to s at time $t+dt$.

Similarly, the atom of probability at zero satisfies the equation

$$\begin{aligned} p_0(t+dt) &= (1 - \lambda dt) p_0(t) + (1 - \lambda dt) \int_0^{\rho(0) dt} p(u, t) du + o(dt) \\ &= (1 - \lambda dt) p_0(t) + p(0, t) \rho(0) dt + o(dt), \end{aligned} \quad (3.4)$$

where the second term on the right-hand side accounts for the probability of moving to $s = 0$ from a value infinitesimally above it, in the absence of rain.

Equations (3.3) and (3.4) are valid for the classical Takács (1955) problem, where the jumps can be of any size, as well as for the present case where the state of the system is bounded by a threshold (i.e. complete saturation at $s = 1$). Here the maximum jump height is bounded and its value depends on the state of the system itself. Such a characteristic does not affect the fact that there is no probability mass for the process at $s = 1$, since the process decays immediately from that state. The reason for this lies in the fact that the input is in the form of an instantaneous pulse rather than a pulse with a finite duration (as in the case considered by Gani (1955)).

A further consequence of the saturation at $s = 1$ is that the right-hand tail of the probability density function of the soil moisture does not necessarily decay to zero, but instead has $p(1, t) > 0$.

Notice that in this analysis, the moisture decay due to losses is of the type $ds/dt = -\rho(s)$, so that if $s(0) = s_0 \leq s^*$ at time $t = 0$ and there is no rain during $(0, t]$, we obtain $s(t) = s_0 e^{-\beta t}$ where β is η/s^* (figure 2). This implies that the dynamics approaches zero asymptotically and thus the process will only be at $s = 0$ if it starts at that value.

Now, if we substitute for Δs and Δz in the right-hand side of (3.3) and neglect all terms of order $o(dt)$, we obtain

$$\begin{aligned} p(s, t + dt) ds &= (1 - \lambda dt) p(s + \rho(s) dt, t) d(s + \rho(s) dt) \\ &\quad + \lambda dt \int_0^s p(z + \rho(z) dt, t) b(s - z; z) d(z + \rho(z) dt) ds \\ &\quad + \lambda dt p_0(t) b(s; 0) ds + o(dt) \\ &= (1 - \lambda dt) \left(p(s, t) + \rho(s) dt \frac{\partial}{\partial s} p(s, t) \right) \left(1 + \frac{\partial}{\partial s} \rho(s) dt \right) \\ &\quad + \lambda dt ds \int_0^s p(z, t) b(s - z; z) dz \\ &\quad + \lambda dt ds p_0(t) b(s; 0) + o(dt). \end{aligned} \quad (3.5)$$

Finally (dividing by ds , subtracting $p(s, t)$ from both sides and dividing by dt , and taking the limit as $t \rightarrow 0$) we obtain

$$\frac{\partial}{\partial t} p(s, t) = \frac{\partial}{\partial s} [p(s, t) \rho(s)] - \lambda p(s, t) + \lambda \int_0^s p(z, t) b(s - z; z) dz + \lambda p_0(t) b(s; 0). \quad (3.6)$$

Similarly, taking the limit as $dt \rightarrow 0$, (3.4) yields

$$\frac{d}{dt} p_0(t) = -\lambda p_0(t) + \rho(0) p(0, t). \quad (3.7)$$

Equations (3.6) and (3.7) are similar to those of Cox & Isham (1986) with the difference that in the present case the jumps of the process are bounded, with an atom of probability at $(1 - s)$. Notice that since the loss function has $\rho(0) = 0$, then from equation (3.7) $p_0(t) = p_0(0) e^{-\lambda t}$ and, as already mentioned, the probability distribution of the soil moisture has no mass at zero except when the process starts at zero.

4. Equilibrium probability distribution of soil moisture

Assuming an equilibrium solution exists, it can be obtained analytically from equations (3.6) and (3.7), by taking the limit as $t \rightarrow \infty$. Setting $p_0(t) = p_0 = 0$, we obtain

$$\frac{d}{ds} [\rho(s) p(s)] - \lambda p(s) + \lambda \int_0^s p(z) b(s - z; z) dz = 0. \quad (4.1)$$

With $b(y; s)$ as given in equation (2.6) we get

$$\frac{d}{ds}[\rho(s)p(s)] - \lambda p(s) + \lambda \gamma e^{-\gamma s} \int_0^s e^{\gamma z} p(z) dz = 0. \quad (4.2)$$

Equation (4.2) was first obtained by Cox & Isham (1986). Multiplying by $e^{\gamma s}$ and differentiating with respect to s , Cox & Isham (1986) obtained the following exact second-order linear differential equation:

$$\frac{d^2}{ds^2}[\rho(s)p(s)] + \gamma \frac{d}{ds}[p(s)\rho(s)] - \lambda \frac{d}{ds}[p(s)] = 0, \quad (4.3)$$

which on integration yields

$$\frac{d}{ds}[\rho(s)p(s)] + \gamma \rho(s)p(s) - \lambda p(s) = \text{const.} \quad (4.4)$$

Setting $s = 0$ in (4.2) gives

$$\frac{d}{ds}[\rho(s)p(s)] - \lambda p(s) = 0$$

at $s = 0$. Since $\rho(0) = 0$, the left-hand side of (4.4) vanishes at $s = 0$, showing that the integration constant is zero.

The general form of the solution is therefore

$$p(s) = \frac{c}{\rho(s)} \exp\left(-\gamma s + \lambda \int \frac{du}{\rho(u)}\right), \quad (4.5)$$

where c is a constant of integration. Because of the form of $\rho(s)$, we consider three different ranges of values for s and choose the corresponding limits of the integral in the right-hand side of equation (4.5) so that $p(s)$ has the same expression at the point defining the ranges regardless of the directions from which these points are approached. In this manner, the general form of the solution is found to be

$$p(s) = \begin{cases} \frac{b}{\rho(s)} \exp\left(-\gamma s + \lambda \int_{s^*}^s \frac{du}{\rho(u)}\right), & 0 < s \leq s^*, \\ \frac{b}{\rho(s)} \exp\left(-\gamma s + \lambda \int_{s^*}^s \frac{du}{\rho(u)}\right), & s^* < s \leq s_1, \\ \frac{b}{\rho(s)} \exp\left(-\gamma s + \lambda \int_{s_1}^s \frac{du}{\rho(u)} + \lambda \int_{s^*}^{s_1} \frac{du}{\rho(u)}\right), & s_1 < s \leq 1. \end{cases} \quad (4.6)$$

After substituting the expressions for the loss function, $\rho(u)$, given by equation (2.9), and working out the integrals, the above equation becomes

$$p(s) = \begin{cases} \frac{c}{\eta} \left(\frac{s}{s^*}\right)^{(\lambda s^*/\eta)-1} e^{-\gamma s}, & 0 < s \leq s^*, \\ \frac{c}{\eta} \exp\left(-\frac{\lambda s^*}{\eta}\right) \exp\left[-s\left(\gamma - \frac{\lambda}{\eta}\right)\right], & s^* < s \leq s_1, \\ \frac{c}{\eta} \left[\frac{k(s-s_1)}{(1-s_1)\eta} + 1\right]^{(\lambda(1-s_1)/k)-1} \exp\left(-\gamma s + \lambda \frac{s_1 - s^*}{\eta}\right), & s_1 < s \leq 1. \end{cases} \quad (4.7)$$

The constant c can be obtained by imposing the requirement

$$\int_0^1 p(s) \, ds = 1. \quad (4.8)$$

It is initially surprising that the atom of probability at $1-s$ in the state-dependent distribution $b(y; s)$ of jumps in soil moisture has not been used explicitly in the above derivation. In fact, the only effect of the saturation of the soil at $s = 1$ is the restricted range over which $p(s)$ is normalized in (4.8). The explanation for this lies in the Markov nature of the soil moisture process. If excursions of the process above unity are impossible, the process will spend more time in states $\{s : s \leq 1\}$ than would be the case otherwise, but the relative proportions of times in those states will be unchanged. For, imagine two processes with, and without, the restriction to $s \leq 1$. In the latter case, trajectories of the soil moisture process will jump above the level $s = 1$ and, eventually, drift down across this level once more. In the former case, these excursions are effectively excised, as the process jumps only to $s = 1$ and then immediately begins its downward decay. The trajectories below $s = 1$ in the two processes are indistinguishable.

The expression for c resulting from the normalizing condition (4.8) is

$$c = \frac{\eta \zeta k e^{\chi} R}{\eta \zeta k (e^{\chi - \gamma s^*} - e^{\lambda s_1 / \eta + \gamma s^*}) + \eta \zeta \xi e^{\vartheta} (1 - s_1) R (\Gamma_2 - \Gamma_1) + \eta k s^* R \Gamma_3}, \quad (4.9)$$

where

$$\left. \begin{aligned} R &= \gamma \eta - \lambda, \quad \zeta = (\gamma s^*)^{\lambda s^* / \eta}, \quad \vartheta = \frac{\gamma \eta (1 - s_1)}{k} + \frac{\lambda s_1}{\eta} + \gamma s^*, \\ \xi &= \left[\frac{\gamma \eta (1 - s_1)}{k} \right]^{-\lambda (1 - s_1) / k}, \quad \chi = \gamma (s_1 + s^*) + \lambda s^* / \eta, \\ \Gamma_1 &= \Gamma[\lambda (1 - s_1) / k, \gamma \eta (1 - s_1) / k], \\ \Gamma_2 &= \Gamma[\lambda (1 - s_1) / k, \gamma (\eta + k) (1 - s_1) / k], \\ \Gamma_3 &= \Gamma[\lambda s^* / \eta, \gamma s^*] \end{aligned} \right\} \quad (4.10)$$

and $\Gamma(a, x)$ stands for the incomplete gamma function.

The expression for the mean

$$\langle s \rangle = \int_0^1 s p(s) \, ds$$

can also be obtained as

$$\begin{aligned} \langle s \rangle &= c \left\{ \left[\varphi_1 \exp \left(-\gamma s_1 + \frac{\lambda}{\eta} (s_1 - s^*) + \gamma s^* \right) - \varphi_2 e^{-\gamma s^*} \right] \right. \\ &\quad \left. + \xi e^{\vartheta - \chi} \frac{1 - s_1}{k} \left[(\Gamma_1 - \Gamma_2) \frac{\eta (1 - s_1) - k s_1}{k} - \frac{1}{\gamma} (\Gamma_4 - \Gamma_5) \right] + \frac{s^*}{\zeta \eta \gamma} \Gamma_6 \right\}, \quad (4.11) \end{aligned}$$

where the new symbols are defined as

$$\left. \begin{aligned} \varphi_1 &= \frac{-\eta - s_1(\gamma\eta - \lambda)}{(\gamma\eta - \lambda)^2}, & \varphi_2 &= \frac{-\eta - s^*(\gamma\eta - \lambda)}{(\gamma\eta - \lambda)^2}, \\ \Gamma_4 &= \Gamma[1 + \lambda(1 - s_1)/k, \gamma\eta(1 - s_1)/k], \\ \Gamma_5 &= \Gamma[1 + \lambda(1 - s_1)/k, \gamma(\eta + k)(1 - s_1)/k], \\ \Gamma_6 &= \Gamma[1 + \lambda s^*/\eta, \gamma s^*]. \end{aligned} \right\} \quad (4.12)$$

Notice that Γ_4 , Γ_5 and Γ_6 are related to Γ_1 , Γ_2 and Γ_3 , respectively (see, for example, Abramowitz & Stegun 1964), but this does not allow for further simplifications.

The variance can also be obtained analytically but it is a long and cumbersome expression which adds little by itself.

5. Impact of climate, soil and vegetation

This section studies the dependence of the equilibrium probability structure of soil moisture on climate, soil and vegetation. The parameters characterizing climate, soil and vegetation were varied over a wide range of values to study the characteristics of the probability density function of relative soil moisture. These ranges were as follows:

rainfall, λ : 2/30–20/30 events day^{-1} ; $1/\alpha$: 2–20 mm event $^{-1}$;

maximum evapotranspiration, E : 2–8 mm day^{-1} ;

soil, nz : 15–80 cm; K_s : 86–13 000 mm day^{-1} ; s^* : 0.15–0.50; s_1 : 0.75–0.90.

The ranges of K_s and s_1 span the extreme conditions of clay and sand soil types. The range of s^* covers conditions that span from herbaceous plants to trees. Since the soil and vegetation parameters are not independent, an auxiliary variable ω has been used that, varying continuously between 0 and 1, links the values of K_s , s^* and s_1 . For simplicity we assume linear relationships between K_s , s^* and s_1 and vary ω to obtain

$$\left. \begin{aligned} K_s &= \omega(K_s^M - K_s^m) + K_s^m, \\ s^* &= \omega(s^{*M} - s^{*m}) + s^{*m}, \\ s_1 &= \omega(s_1^M - s_1^m) + s_1^m. \end{aligned} \right\} \quad (5.1)$$

The symbols ‘M’ and ‘m’ stand for the maximum and minimum values of the ranges used for the parameters. Equation (5.1) has no physical significance and is merely a device to simplify the choices of sets of parameter values. It is also useful for the graphical representation of the results.

Figure 3*a–d* shows examples of the equilibrium probability density of soil moisture at a point, under different conditions. It is interesting to notice the drastically different shapes the density may take, depending on climate, soil and vegetation characteristics. The first case (figure 3*a*) refers to a situation typical of a tropical climate with very frequent rainfall of moderate intensity, where the soil is quite deep and vegetation gives a high value of maximum evapotranspiration because of the high average temperature. In such a case the density is concentrated around values of soil moisture just below s_1 . Above s_1 , leakage quickly becomes dominant—and this is true for all four cases—preventing soil moisture from reaching values close to saturation for any

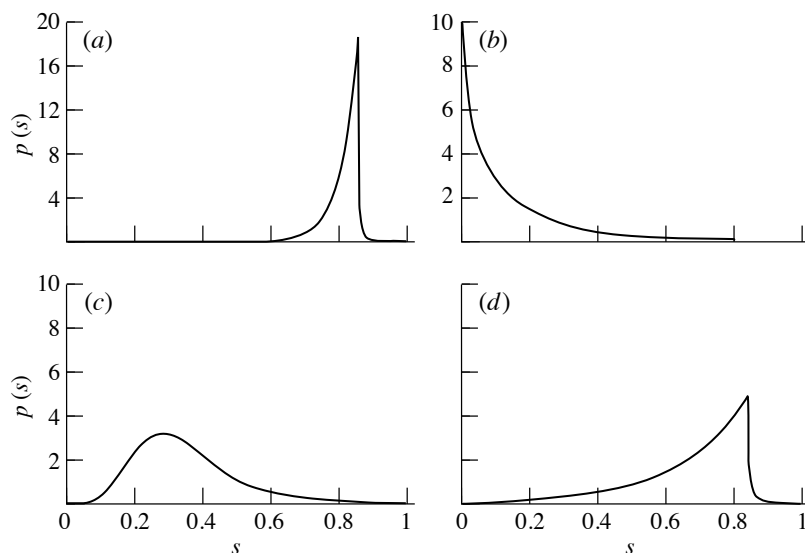


Figure 3. Examples of the equilibrium density of soil moisture at a point under different conditions of soil, rainfall, and evapotranspiration. (a) Mean rainfall depth, $1/\alpha = 15 \text{ mm event}^{-1}$; rainfall rate, $\lambda = 2/3 \text{ events day}^{-1}$; evapotranspiration rate, $E = 6 \text{ mm day}^{-1}$; saturated hydraulic conductivity, $K_s = 900 \text{ mm day}^{-1}$; relative soil moisture below which evapotranspiration is less than the maximum, $s^* = 0.3$; value at which the unsaturated hydraulic conductivity is conventionally (figure 2) set to zero, $s_1 = 0.85$; effective soil depth available to water, $nz = 45 \text{ cm}$. (b) $1/\alpha = 20 \text{ mm event}^{-1}$; $\lambda = 1/10 \text{ events day}^{-1}$; $E = 6 \text{ mm day}^{-1}$; $K_s = 5000 \text{ mm day}^{-1}$; $s^* = 0.45$; $s_1 = 0.8$; $nz = 10 \text{ cm}$; (c) $1/\alpha = 10 \text{ mm event}^{-1}$; $\lambda = 1/6 \text{ events day}^{-1}$; $E = 2.5 \text{ mm day}^{-1}$; $K_s = 200 \text{ mm day}^{-1}$; $s^* = 0.3$; $s_1 = 0.9$; $nz = 20 \text{ cm}$. (d) $1/\alpha = 20 \text{ mm event}^{-1}$; $\lambda = 1/3 \text{ events day}^{-1}$; $E = 4 \text{ mm day}^{-1}$; $K_s = 300 \text{ mm day}^{-1}$; $s^* = 0.3$; $s_1 = 0.85$; $nz = 30 \text{ cm}$.

significant periods and thus making irrelevant the probability density above s_1 . The consistent losses, especially from evapotranspiration, are abundantly compensated by the frequent precipitation that ensures almost constant middle-to-high values of soil moisture that are ideal for a thriving vegetation. Case (b) is typical of a hot arid region with shallow sandy soil and a mixture of trees, shrubs and grasses. Values of maximum evapotranspiration are still high for all the species, but now the value of s^* is higher because grasses and desert shrubs start experiencing stress when soil moisture levels are still quite high due to the faster control of their stomata. Clearly, in this case, the density is concentrated at very low values of s and the vegetation, which is very frequently under stress, can survive only because of its very low wilting points. Figure 3c applies to a cold region with an arid climate and very low values of maximum evapotranspiration due to the low temperature. The soil moisture density is more open with middle-low average values. Finally, case (d) shows the density for a forest in a temperate region. The shape of the density recalls that of the tropical forest, but with a less pronounced peak at high soil moisture values. The vegetation is usually in good condition but may also experience some periods of stress. From the analysis of figure 3a–d we notice that the variety of shapes makes it unlikely that they can be accommodated by adjusting a common distribution (e.g. gamma) with different moments.

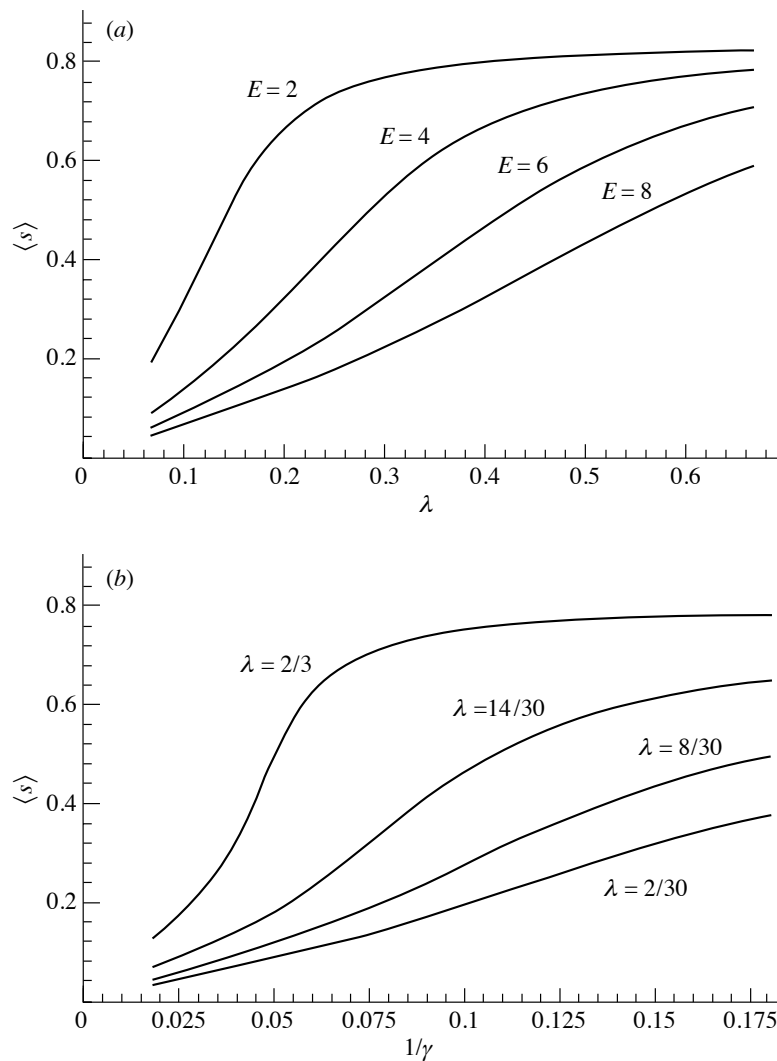


Figure 4. Mean equilibrium soil moisture versus climate parameters for a given type of soil ($K_s = 1000 \text{ mm day}^{-1}$, $s^* = 0.35$, $s_1 = 0.85$, $nz = 15 \text{ cm}$). (a) Mean equilibrium soil moisture versus rate of storm arrivals, λ , plotted for different values of evapotranspiration rate in mm day^{-1} . (b) Mean equilibrium soil moisture versus normalized mean rainfall depth, $1/\gamma$, plotted for different values of the rate of storm arrivals.

Figure 4a,b shows the mean equilibrium soil moisture plotted in two different manners emphasizing the impact that evapotranspiration, rate of storm arrivals and mean depth per event have in controlling the mean soil moisture. The soil characteristics are taken in the middle range of their possible values. Notice the change in the rising limb of the relationship. When rain events occur very frequently, the mean value of the soil moisture becomes highly dependent on the mean depth of the storms up to a point, after which it remains practically constant and close to saturation.

Figure 5 shows the mean soil moisture as a function of soil characteristics—

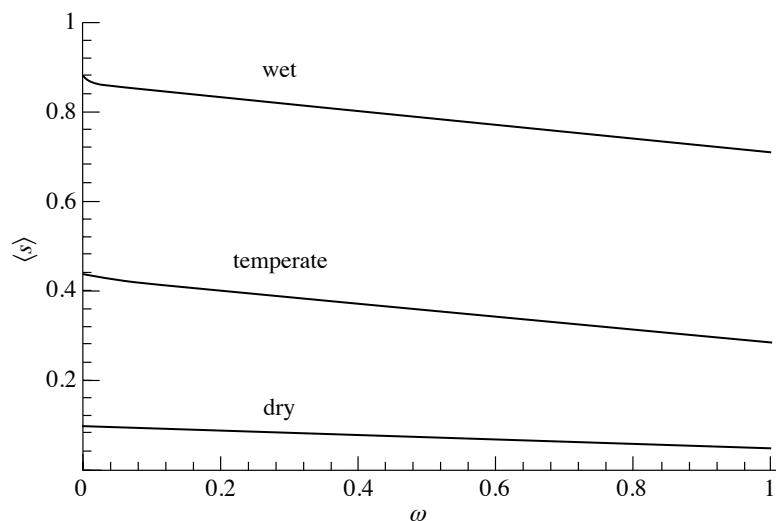


Figure 5. Mean equilibrium soil moisture plotted as a function of soil characteristics using the auxiliary variable ω defined in equations (5.1). The three curves refer to three different climate conditions loosely designated as wet ($E = 3 \text{ mm day}^{-1}$, $\lambda = 2/3 \text{ events day}^{-1}$, $1/\alpha = 20 \text{ mm event}^{-1}$), temperate ($E = 5 \text{ mm day}^{-1}$, $\lambda = 8/30 \text{ events day}^{-1}$, $1/\alpha = 15 \text{ mm event}^{-1}$) and dry ($E = 7 \text{ mm day}^{-1}$, $\lambda = 4/30 \text{ events day}^{-1}$, $1/\alpha = 10 \text{ mm event}^{-1}$).

embedded in the auxiliary variable ω —for climates loosely designated as wet, temperate and dry. We see that, for the dry climate, the variation in soil properties has very little impact as the mean soil moisture decreases only in a very narrow range. For the wet and temperate climates there are more pronounced effects, which are similar in both cases, in terms of the relative changes produced. These results somewhat resemble the findings of Schaap *et al.* (1997) for forest floor water content where simple linear relationships seem adequate to translate water content from one site to another.

The variance of the soil moisture equilibrium density is shown in figure 6*a, b* for a fixed set of soil conditions as functions of the characteristics of rainfall and evapotranspiration. Again we can observe the dramatic changes that the variance undergoes when λ , η or γ is changed. It is interesting to point out that, except for very dry climates, the variance of the soil moisture has a well-defined maximum. Thus for a given mean frequency of rain events, the variance increases with increasing mean soil depth up to a point, after which any further increase in mean depth leads to a decrease in variance; this is because most of the distribution becomes concentrated on high values of relative soil moisture. The point at which the maximum occurs varies with the frequency of events and is also a function of the soil and vegetation parameters. Figure 7 shows the dependence of the variance on soil characteristics represented by the auxiliary variable ω for three climates loosely designated as wet, temperate and dry.

6. Average water balance

The purpose of this section is to represent the different components of the water balance dynamics at a point under different conditions of climate, soil and vegeta-

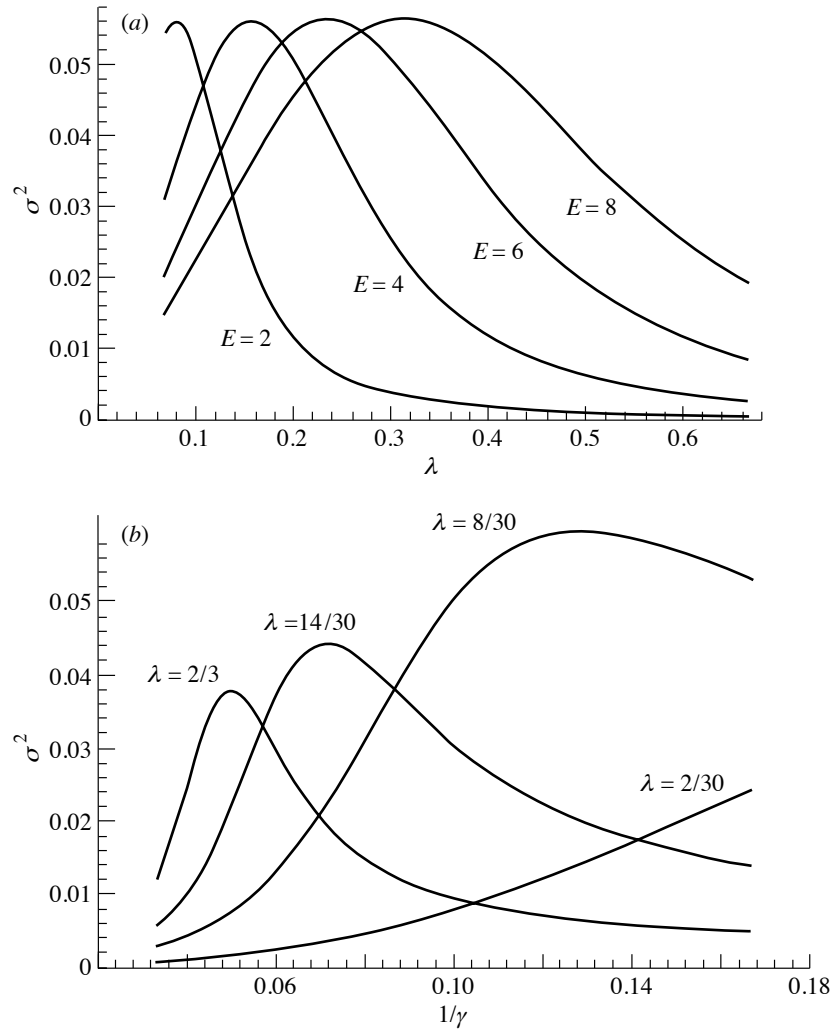


Figure 6. Variance of the soil moisture equilibrium density shown as a function of climate parameters for a given type of soil ($K_s = 1000 \text{ mm day}^{-1}$, $s^* = 0.35$, $s_1 = 0.85$). (a) Variance versus rate of storm arrivals, λ , plotted for different values of evapotranspiration rate in mm day^{-1} . (b) Variance versus normalized mean rainfall depth, $1/\gamma$, plotted for different values of rate of storm arrivals.

tion. For purposes of soil water dynamics, four different types of water losses will be considered at a site: evapotranspiration when vegetation is under stress, evapotranspiration without vegetation stress, leakage and run-off.

The mean values of the first three types of losses are described in normalized form (i.e. divided by nz) through the equation

$$\int_0^1 \rho(s)p(s) ds = \int_0^{s^*} \beta sp(s) ds + \int_{s^*}^{s_1} \eta p(s) ds + \int_{s_1}^1 \frac{k(s-s_1)}{1-s_1} p(s) ds, \quad (6.1)$$

where $\beta = \eta/s^*$ and other terms were defined in equation (2.9). The three terms on

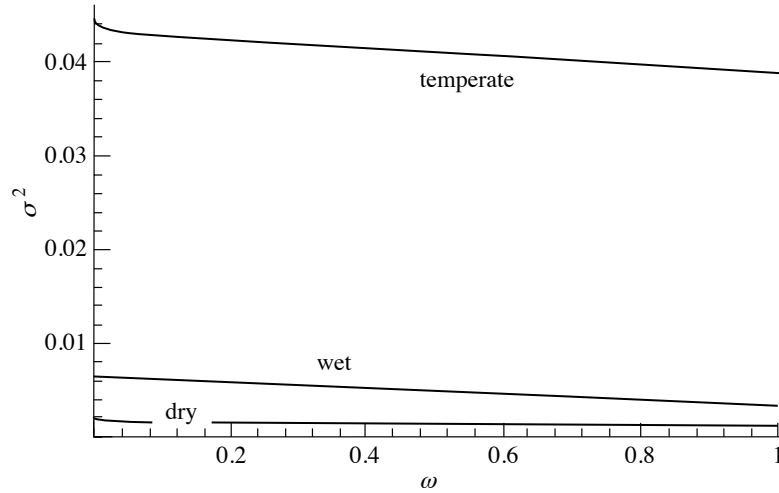


Figure 7. Variance of the soil moisture equilibrium density plotted as a function of soil characteristics using the auxiliary variable ω defined in equation (5.1). The three curves refer to three different climate conditions loosely designated as wet ($E = 3 \text{ mm day}^{-1}$, $\lambda = 2/3 \text{ events day}^{-1}$, $1/\alpha = 20 \text{ mm event}^{-1}$), temperate ($E = 5 \text{ mm day}^{-1}$, $\lambda = 8/30 \text{ events day}^{-1}$, $1/\alpha = 15 \text{ mm event}^{-1}$) and dry ($E = 7 \text{ mm day}^{-1}$, $\lambda = 4/30 \text{ events day}^{-1}$, $1/\alpha = 10 \text{ mm event}^{-1}$).

the right-hand side of equation (6.1) will be denoted by $\langle e_s \rangle$, $\langle e_{ns} \rangle$ and $\langle l \rangle$, and their sum by $\langle L \rangle$.

The mean surface run-off is given in normalized form (i.e. normalizing by nz) by

$$\langle q \rangle = \langle i \rangle - \int_0^1 \rho(s)p(s) \, ds, \quad (6.2)$$

where $\langle i \rangle$ is the normalized mean rainfall intensity

$$\langle i \rangle = \lambda/\gamma, \quad (6.3)$$

where γ was defined as αnz .

The integration of equation (6.1) gives the following expressions for the normalized components of the average water balance dynamics:

$$\left. \begin{aligned} \langle e_s \rangle &= c \frac{\Gamma_6}{\gamma \zeta}, \\ \langle e_{ns} \rangle &= \frac{c}{\gamma \eta - \lambda} [\eta e^{-\gamma s^*} - e^{-\gamma s_1 + \lambda(s_1 - s^*)/\eta}] + c \xi \frac{\eta}{k} (1 - s_1) (\Gamma_2 - \Gamma_1) e^{\vartheta - \chi}, \\ \langle l \rangle &= c \xi \frac{s_1}{k} (\Gamma_2 - \Gamma_1) e^{\vartheta - \chi} + c \frac{\xi}{k} \left[\left(\frac{\eta(1 - s_1)}{k} - s_1 \right) (\Gamma_2 - \Gamma_1) + (\Gamma_6 - \Gamma_5)/\gamma \right] e^{\vartheta - \chi}. \end{aligned} \right\} \quad (6.4)$$

Figure 8*a, b* shows the normalized component of the mean water balance for some specific values of rainfall, soil and vegetation characteristics. As expected all the components are strongly affected by rainfall and evapotranspiration. Soil characteristics are also quite important. The leakage is in relative terms smaller than the other components, although it may be considerable for high values of K_s .

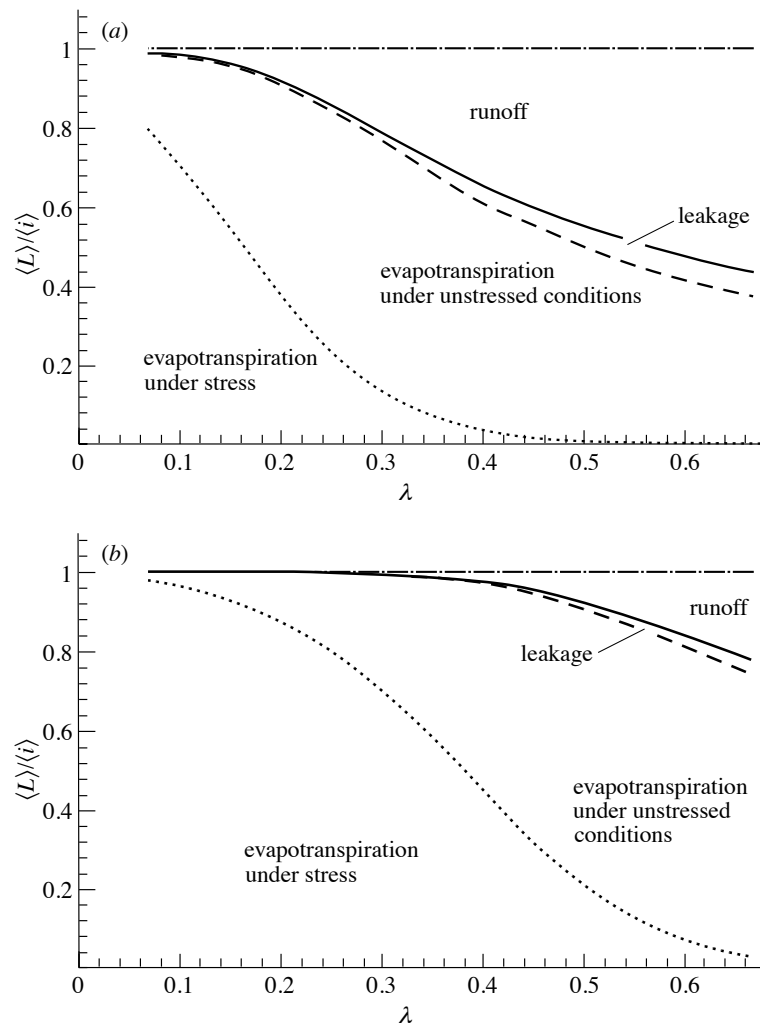


Figure 8. Mean water balance for a given type of soil ($K_s = 1000 \text{ mm day}^{-1}$, $s^* = 0.35$, $s_1 = 0.85$, $nz = 15 \text{ cm}$) in two different climate conditions: (a) $1/\alpha = 20 \text{ mm day}^{-1}$, $E = 5 \text{ mm day}^{-1}$; (b) $1/\alpha = 10 \text{ mm day}^{-1}$, $E = 5 \text{ mm day}^{-1}$.

7. Concluding remarks

In this paper we have studied the main properties of the probability distribution of soil moisture at a site when both the input into the soil from rainfall as well as the losses from evapotranspiration and leakage are dependent on the moisture state of the soil. It has been shown that climate, soil and vegetation have a dramatic effect on the shape and moments of the soil moisture distribution to the extreme that it is unlikely that it can be adequately represented by any of the commonly used probability density functions. The direction for further developments is oriented towards inclusion of spatial dynamics arising mainly from competition for soil moisture by neighbouring plants.

References

- Abramowitz, M. & Stegun, I. A. 1964 *Handbook of mathematical functions*. New York: Dover.
- Clapp, R. B. & Hornberger, G. N. 1978 Empirical equations for some soil hydraulic properties. *Water Resources Res.* **14**, 601–604.
- Cox, D. R. & Isham, V. 1986 The virtual waiting-time and related processes. *Adv. Appl. Prob.* **18**, 558–573.
- Cox, D. R. & Miller, H. D. 1965 *The theory of stochastic processes*. London: Methuen.
- Dunne, T. 1978 Field studies of hillslope flow processes. In *Hillslope hydrology* (ed. M. J. Kirkby), pp. 227–293. New York: Wiley-Interscience.
- Eagleson, P. S. 1982 Dynamic hydro-thermal balance at macroscale. In *Land surface processes in atmospheric general circulation models* (ed. P. S. Eagleson), pp. 289–357. Cambridge University Press.
- Entekhabi, D. & Rodriguez-Iturbe, I. 1994 Analytical framework for the characterization of the space-time variability of soil moisture. *Adv. Water Resources* **17**, 35–45.
- Gani, J. 1955 Some problems in the theory of provisioning and of dams. *Biometrika* **42**, 179–200.
- Milly, P. C. D. 1993 An analytic solution of the stochastic storage problem applicable to soil water. *Water Resources Res.* **29**, 3755–3758.
- Rodriguez-Iturbe, I., Entekhabi, D. & Bras, R. L. 1991 Non-linear dynamics of soil moisture at climatic scales. I. Stochastic analysis. *Water Resources Res.* **27**, 1899–1906.
- Schaap, M. G., Bouten, W. & Verstaten, J. M. 1997 Forest floor water content dynamics in a Douglas fir stand. *J. Hydrol.* **201**, 367–383.
- Scholes, R. J. & Walker, B. H. 1993 *An African savanna*. Cambridge University Press.
- Takács, L. 1955 Investigation of waiting-time problems by reduction to Markov processes. *Acta Math. Acad. Sci. Hungar.* **6**, 101–129.

